Performance improvement for optimization of non-linear geometric fitting problem in manufacturing metrology*

Giovanni Moroni,Wahyudin P. Syam, and Stefano Petrò
Mechanical Engineering Department, Politecnico di Milano, Via La Masa 1, 20156 Milan, Italy

Abstract

Product quality is a main concern in today manufacturing. It is a fundamental requirement for companies to be competitive. To assure such quality, a dimensional inspection to verify geometric property of a product has to be carried out. High speed non contact scanners help this task, by both speeding up acquisition speed and increasing accuracy through a more complete description of the surface. The algorithms for the management of the measurement data play a critical role in ensuring both the measurement accuracy and speed. One of the most fundamental parts of the algorithm is procedure for fitting substitute geometry to the cloud of points. This article addresses this challenge. Three relevant geometries are selected as case studies: non-linear least-square fitting of circle, sphere and cylinder. These geometries are chosen with consideration of their common use in practice; for example the sphere is often adopted as reference artifact for performance verification of coordinate measuring machine (CMM) and cylinder is the most relevant geometry for pin-hole relation as an assembly feature to construct a complete functioning product.

In this article, an improvement of the initial point guess for Levenberg-Marquardt (LM) algorithm by employing Chaos Optimization (CO) method is proposed. This causes a performance improvement in the optimization of a non-linear function fitting the three geometries. The results show that, with this combination, higher quality of fitting results in term of smaller norm of the residuals can be obtained while preserving the computational cost. Fitting a "incomplete-point-cloud", which is a situation where the point cloud do not cover a complete feature e.g. from half of the total part surface, is also investigated. Finally, a case study about fitting a hemisphere is presented.

Keywords: Least-square fitting, non-linear optimization, multi-modal function, steepest-decent, Gauss-Newton, chaos search.

** This is an extended article that were presented as keynote paper at IMEKO 11th ISMQC 2013, Cracow-Kielce, Poland.*
Corresponding author: Wahyudin P. Syam (wahyudinpermana.syam@polimi.it

1. Introduction

Quality of manufacturing product is the main concern in modern world to increase competitiveness [1]. Quality inspection is the procedure to verify this geometric attribute and can

be realized by dimensional metrology [2]. In dimensional metrology, least-square (LS) fitting of substitute geometries, after obtaining measurement points, is a fundamental step before any geometric feature may be evaluated [3],[4],[5],[6]. LS fitting algorithm from points cloud to basic geometric feature is deployed after obtaining a set of measured points. Hence, the dimensional measurement, such as the diameter of a circle or sphere, the angle between two lines, the distance between two axes, etc, can be evaluated (fig. 1). Subsequently, a routine for fitting task is a critical element in the chain of dimensional metrology for quality inspection. In this case, fitting the substitute geometry is called function reconstruction [7]. The lack of prior knowledge about the nominal geometry to be fitted can significantly increase the difficulties in the fitting itself. For example, a lack of prior knowledge about the direction of the axis of a cylinder significantly increases the difficulty of the identification of the real axis direction. This is the usual condition of reverse engineering. In addition to the difficulties of fitting process, a fast fitting process is a stringent requirement since recent measurement instruments are able to obtain rapidly thousands or even millions of points in few seconds. In this case, fitting time can significantly increase the overall measurement time, but high-speed inspection is required to reduce the inspection cost, and in general, to reduce the product cost [8]. Hence, an accurate and high-speed fitting procedure is a strict requirement.

In the case of linear least squares fitting (like e.g. in the case of plane fitting) robust solutions are available. These solutions are based on finding the direction cosine of a line or plane from the Eigen vectors of the cloud of points. The eigenvectors correspond to its highest and smallest singular value, which can be calculate by means of the Singular Value Decomposition (SVD), for which fast and reliable algorithms are commonly available [6]. But, in the case of non-linear least squares fitting (like e.g. in the case of circle, sphere and cylinder fitting) such simple solutions are not available. This paper will propose an improvement of the current state of art in the field of non-linear least squares fitting of geometries. The improvement is based on a wise choice of the initial solution thanks to the application of Chaos Optimization (CO). The optimal initial solution will be coupled to a standard (e.g. Levenberg-Marquardt) nonlinear least squares optimization algorithm for finding the final fitting geometry. The effectiveness of the proposed approach will be compare to the standard use of Levenberg-Marquardt algorithm in the case of sphere, cylinder, and circle fitting.

2. Non-linear Fitting

Basic substitute geometries are divided in two groups: linear and non-linear geometry. This grouping criterion is based on their defined parameters. Line (2D and 3D) and plane fall into linear geometry, as their parameters can be estimated by means of linear least squares fitting. On the other hand, other basic geometry such as circle, sphere, cylinder, cone and torus have non-linear parameters defining their shapes. Subsequently, they are categorized as non-linear geometries. LS fitting of circle, sphere and cylinder will be addressed in this article. Circle and sphere geometries have many applications, for example sphere is a common artifact geometry for calibration of dimensional metrology instruments [9],[10]. In addition, many mechanical products have rotational functionality which is constituted by circular from shafts and holes. Cylinder is a geometry representation of these shaft-hole systems [11].

The basis of LS fitting is the minimization of an objective function constituted by a sum of square of errors. Error is defined as the difference between estimated and measured value. In dimensional metrology, error is usually assimilated to the local geometrical deviation, i.e. the distance between measured points and ideal substitute geometry (fig 2). LS fitting objective function is defined as:

$$\arg\min_{\mathbf{p}} F\left(\mathbf{p},\mathbf{x}_i\right)=\sum_{i=1}^{n} d_i^2\left(\mathbf{p}\right) \tag{1}$$

Where: F is the distance function of points $\boldsymbol{x}$ to the fitted geometry. $\mathbf{x}_i$ is a cloud of n points sampled on a surface and $\mathbf{p}$ is set of parameters on which a distance function $d_i\left(\mathbf{p}\right)$ depends on, so that $d_i\left(\mathbf{p}\right)$ is the distance of the i-th point from the substitute geometry defined by $\mathbf{p}$. For the circle, the distance function is (Fig. 2a left):

$$d_i\left(\mathbf{x}_0,r\right)=\left\|\mathbf{x}_i-\mathbf{x}_0\right\|-r=\sqrt{\left(x_i-x_0\right)^2+\left(y_i-y_0\right)^2}-r \tag{2}$$

Where $\mathbf{x}_0=\left[x_0,y_0\right]^{\mathrm{T}}$ is the circle center, r is the circle radius, and $\mathbf{x}_i=\left[x_i,y_i\right]^{\mathrm{T}}$ is the i-th point, and $\left\|\mathbf{x}\right\|$ is L_2-norm of a vector $\mathbf{x}$, e.g. $\left\|\mathbf{v}\right\|=\sqrt{v_i^2+v_2^2+v_3^2}$.

Similarly, for the sphere, the function can be formulated as:

$$d_i\left(\mathbf{x}_0,r\right)=\left\|\mathbf{x}_i-\mathbf{x}_0\right\|-r=\sqrt{\left(x_i-x_0\right)^2+\left(y_i-y_0\right)^2+\left(z_i-z_0\right)^2}-r \tag{3}$$

Where $\mathbf{x}_0=\left[x_0,y_0,z_0\right]^{\mathrm{T}}$ is the sphere center, r is the sphere radius, and $\mathbf{x}_i=\left[x_i,y_i,z_i\right]^{\mathrm{T}}$ is the *i*-th point.

The distance function of a point to a cylinder is more complex (see fig. 2a right):

$$d_i\left(\mathbf{x}_0,\mathbf{n},r\right)=d_{i(3dp2Axis)}-r=\frac{\left\|\left(\mathbf{x}_i-\mathbf{x}_0\right)\times\mathbf{n}\right\|}{\left\|\mathbf{n}\right\|}-r \tag{4}$$

where r is the radius of the cylinder and $d_{i(3dp2Axis)}$ is defined as distance between 3D point $\boldsymbol{x_i}$ to the axis of cylinder (a straight line). The axis is defined by a point $\mathbf{x}_0$ belonging to it and a direction vector $\mathbf{n}$ (fig. 2b).

One can observe that the objective function *F* which has to be minimized is a non-linear multi-modal function which has many local minima and/or maxima.

3. Levenberg-Marquardt Algorithm.

Levenberg-Marquardt (LM) algorithm is a well-known approximation method for solving non-linear least square problems that has applications in many fields [12, 13]. The recipe of LM algorithm is the blending between steepest-decent (gradient search) step method and Gauss-Newton step method. When the current solution is far from the optimal, the LM method acts like a steepest-decent method. Then, LM method will become a Gauss-Newton when the solution is near optimal. The basis of steepest-decent method is searching with regard to the direction of the gradient. Let F be the function to optimize, and x_k the candidate solution at step k. Since in this case minimization is the problem to solve, the next step in the searching procedure is:

$$x_{k+1} = x_k - \lambda_s \nabla F \tag{5}$$

Where $\nabla F = (\partial F / \partial x, \partial F / \partial y, \partial F / \partial z)$ is the gradient of the objective function as well as the search direction, and λ_s is the step size which determines how far the next candidate solution will be from the current one. Hence, if the λ_s value is set very small, then it will take longer to reach convergence. Otherwise, if the value of λ_s is very large, there is a high probability that the searching process will over-step the optimum value. In Gauss-Newton method, linearization by using Taylor expansion series is deployed. The series are $\nabla \mathrm{f}(\mathbf{p}) = \nabla \mathrm{f}(\mathbf{p}_0) + (\mathbf{p} - \mathbf{p}_0)^{\mathrm{T}} \nabla^2 \mathrm{f}(\mathbf{p}_0) + \underbrace{\ldots + \left[(\mathbf{p} - \mathbf{p}_0)^{\mathrm{T}}\right]^{\mathrm{n}} \nabla^{\mathrm{n}} \mathrm{f}(\mathbf{p}_0)}_{\text{Higher order term}}$. Commonly, higher order expansions are not considered. Not only the algorithm is more efficient to reach the convergence, but also the form is tractable to solve $\mathbf{p}$. By setting $\nabla \mathrm{f}(\mathbf{p}) = 0$, the next step of the Gauss-Newton can be calculated as:

$$\mathbf{p}_{j+1} = \mathbf{p}_j - \left(\mathbf{J}_{\mathbf{d}}^{\mathrm{T}} \mathbf{J}_{\mathbf{d}}\right) \mathbf{J}_{\mathbf{d}}^{\mathrm{T}} \mathbf{d}\left(\mathbf{p}_j\right) \tag{6}$$

Where $\mathbf{d}\left(\mathbf{p}_j\right)$ is the vector of the residual (distances) at step j, and $\mathbf{J}_{\mathbf{d}}$ is the Jacobian matrix of this vector of distance functions. Note that Taylor expansion series is accurate only for a small range of region, called trust region. This small region is a region where the non-linear estimation of a function by using Taylor expansion is still reasonably valid. It implies that Gauss-Newton method is valid for searching through a small area of the neighborhood. Subsequently, the method is effective when the initial guess is near the optimum solution.

LM method combines the advantages of steepest-decent and Gauss-Newton methods. A vector of input parameters $\mathbf{p}_0$, which includes the parameters that will be optimized, is supplied to the LM algorithm, along with matrix ***M*** which is A $n \times 3$ matrix of all the data points, defined as: $\left[x_1 \;\; y_1 \;\; z_1; \;\ldots\; \ldots\; \ldots; x_n \;\; y_n \;\; z_n\right]$, so that an optimized vector of parameters $\mathbf{p}$ is obtained. The LM method used here is based on the LM used by NIST [6] for their algorithm testing system. The LM algorithm is:

Algorithm 1: Levenberg-Marquardt Algorithm

Input: Vector $\mathbf{p}_0$ which is the initial guess for the parameter and matrix ***M*** which is the point cloud to be fitted.
Output: Vector $\mathbf{p}$ which is the fitted parameter

1: Set $\lambda = 0.0001$
2: DO { decrease λ
3: set $\mathbf{U} = \mathbf{J}_0^{\mathrm{T}}\mathbf{J}_0$
4: set $\mathbf{v} = \mathbf{J}_0^T\mathbf{d}(\mathbf{p}_0)$
5: set $F_0 = \mathbf{d}^{\mathrm{T}}(\mathbf{p}_0)\mathbf{d}(\mathbf{p}_0)$
6: DO { increase λ
7: set $\mathbf{H} = \mathbf{U} + \lambda(\mathbf{I} + \mathrm{diag}(\mathbf{U}))$
8: solve $\mathbf{Hx} = -\mathbf{v}$
9: set $\mathbf{p}_{new} = \mathbf{p}_0 + \mathbf{x}; set\ F = \mathbf{d}^{\mathrm{T}}(\mathbf{p}_{new})\mathbf{d}(\mathbf{p}_{new})$
10: IF converged THEN return $\mathbf{p}_0 = \mathbf{p}_{new}$
11: UNTIL $F_{new} < F_0$ or stop criterion is *true*
12: IF $F_{new} < F_0$ THEN $\mathbf{p}_0 = \mathbf{p}_{new}$
13: UNTIL stop criterion is *true*

λ is LM variable, which is increased and decreased by 10 and 0.04, respectively, according to NIST suggestion [6]. $\mathbf{J}_0$ is a Jacobian matrix which elements on its *i*-th row are $\nabla d_i(\mathbf{p}_0)$, which are the first order partial derivatives of d_i respect to each parameter which has to be estimated for each *i*-th point. For circle, the parameters $\mathbf{p}_0$ are x_0, y_0 of its center and radius r. For sphere, only one additional element z_0 for its 3D position of the center is added to the parameters. Finally, the parameters for cylinder are x_0, y_0, z_0 which is a point on the axis, having vector of cosine direction (normal) $\boldsymbol{n}$ $(\boldsymbol{n}_1, \boldsymbol{n}_2, \boldsymbol{n}_3)$, and finally its radius r. The number of column of matrix $\mathbf{J}_0$ corresponds to the number of parameters to be estimated, and the number of rows corresponds to number of points the substitute geometry will be fitted to.

The central idea of this LM method lies on the equation $\mathbf{Hx} = \mathbf{-v}$. If this equation is enlarged into $\mathbf{J}_0^T\mathbf{J}_0 + \lambda(\mathbf{I} + \mathrm{diag}(\mathbf{J}_0^T\mathbf{J}_0)\mathbf{x}) = -\mathbf{J}_0^T\mathbf{d}(\mathbf{p}_0)$, one can observe that if λ is zero or small, LM behavior become Gauss-Newton method. In the opposite, if λ is large, then the off-diagonal elements of $\mathbf{J}_0^T\mathbf{J}_0$ will have less effect such that LM behaves like steepest-decent method. The term $\mathbf{I} + diag(\mathbf{J}_0^T\mathbf{J}_0)$ is used instead of $\mathbf{D}^T\mathbf{D}$. This is a weighted distance matrix (depending on the geometry which will be estimated), based on Nash [13] suggestion, such that $\mathbf{Hx} = \mathbf{J}_0^T\mathbf{J}_0 + \lambda(\mathbf{I} + \mathrm{diag}(\mathbf{J}_0^T\mathbf{J}_0)\mathbf{x}) = -\mathbf{J}_0^T\mathbf{d}(\mathbf{p}_0)$ becomes positive definite.

4. Initial Point Problem

LM iterative method mentioned in the previous section depends significantly on the initial guess of a set of solutions, $\mathbf{p}_0$ [14]. This situation is similar to any other iterative algorithm. The function to be optimized is a multi-modal function with a complex contour and many local optimums. Subsequently, the risk exists that the search is trapped in a local optimum region. The

illustration of multi-model function is shown in fig. 3 (left) by using Schweifel function and square of the summation of a circle distance function, which is $F = \sum_{i=1}^{N} d_i^2$, where d_i is declared in equation (2).

As mentioned before, the LS nonlinear function which to be minimized to fit geometries is multi modal. Hence, it has many local minima, only one being the global optimum. If the optimization process gives a local minimum solution, then the solution is sub-optimal. The searching procedure can be trapped in local minima depending on where the initial guess is put. Subsequently, as it can be presumed, the result is significantly affected by the initial guess [14]. For example, the objective function to fit a circle is shown in fig. 3 (right). The surface is constructed by varying the (x, y) center position of the circle. The different colors show how the surface changes as the candidate radius r changes. Even though in this case the optimization zone is convex, different levels of radius r create different separated optimization zones. This can trap the searching process in one of the optimization zones. Therefore, it is possible the final solution is not a global optimum, depending on the initial solution. Fig. 4 illustrates how initial guess as starting solution affects the final results. If the initial guess is far from optimum, an unexpected final result can be obtained (fig. 4a). On the other hand, a good initial guess significantly improves the final solution reducing the objective function value (fig. 4b).

5. Chaos Optimization

Chaos is defined as a semi-randomness property. This property is generated by a nonlinear deterministic equation. It creates a chaotic dynamic step which can easily escape from local optima. The concept is different with using rejection-accepting probability test in random-based algorithms, such as improvement heuristic search [15]. Searching through regularity of chaotic motion, represented by one-dimensional logistic map, is its fundamental recipe [16]. Chaos optimization (CO) uses these chaos properties, which are ergodicity, stochastic property, and regularity [17]. The one-dimensional logistic map used is:

$$\mathbf{t}_{k+1} = \lambda_c \mathbf{t}_k (1 - \mathbf{t}_k) \tag{7}$$

Where $\lambda_c \in \{3.56, 4\}$ is a control argument and k is iteration number. Yang [18] recommended $0 \le \mathbf{t}_0 \le 1$ where $\mathbf{t}_0 \notin \{0, 0.25, 0.5, 0.75, 1.0\}$. The behavior of equation (7) becomes chaotic in the sense that its value is drastically changed within the limit of λ_c and $\mathbf{t}_k$ presenting the regularity of chaotic motion. Fig. 5 shows the plot of time series of this function and paired-plot between two consecutive chaos variables.

This CO is used to improve the initial guess of LM non-linear fitting iterative method, so that the initial guess is near the optimal solution, thus preserving the computation time, which is very important when the sample size is large (millions of points). The combination of CO algorithm with LM algorithm to improve the initial guess is as follows:

Algorithm 2: Chaos search to improve the initial guess in LM method

Input: Vector $\mathbf{p}_0$ is the initial guess for the parameter (1:*n-param*)

Goal: New vector $\mathbf{p}_0$ is the improved initial guess by

$Min\, F(\mathbf{p}_i)$, $\mathbf{p}_i \in \{\mathbf{a}_i, \mathbf{b}_i\}$, $Let\, \mathbf{p}^k = (\mathbf{p}^1 : \mathbf{p}^k)$, $\mathbf{t}^k = (\mathbf{t}^1 : \mathbf{t}^k)$

$where: \mathbf{p} = (p_1,..., p_n)\ and\ \mathbf{t} = (t_1,..., t_n)$

1: Set $k = 0, r = 0$, Set $k_{\max} = 10, r_{\max} = 30$

2: Produce randomly. $\mathbf{t}_0 \in \{0,1\}\ and \notin \{0,0.25,0.5,0.75,1.0\}$.

3: Set $\mathbf{t}^k = \mathbf{t}^0, \mathbf{t}^* = \mathbf{t}^0, \mathbf{a}^0 = \mathbf{p} - MPE, \mathbf{b}^0 = \mathbf{p} + MPE$
where :$\mathbf{a} = (a_i,..., a_n)$, $\mathbf{b} = (b_i,..., b_n)$

4: Set $\mathbf{p}^* = \mathbf{p}_0 \rightarrow$ **initial guess parameter**

5: DO WHILE { $r < r_{\max}$;
DO WHILE { $k < k_{\max}$;

6: Set $p_i = a_i^r + t_i^r (b_i^r - a_i^r)$;
calculate $F^k = \sum_{i=0}^{N} d_i^2 (p_i)$

7: IF $F^k < F^*$ THEN
$F^* = F(p^k), p^* = p^k, t^* = t^k$

8: $k = k + 1$; $t_i^k = \lambda t_i^{k-1}(1 - t_i^{k-1}), \lambda \in \{3.56,4\}$

9: } END *k*-th iteration; $r = r + 1$

$a_i^{r+1} = p_i^* - \gamma(b_i^r - a_i^r)$

10: and

$b_i^{r+1} = p_i^* + \gamma(b_i^r - a_i^r)$

11: IF $a_i^{r+1} > a_i^r$ THEN $a_i^{r+1} = a_i^r$, $\gamma \in \{0,0.5\}$

12: IF $b_i^{r+1} < b_i^r$ THEN $b_i^{r+1} = b_i^r$, $\gamma \in \{0,0.5\}$

13: IF $r < r_{\max}$ THEN produce $t_0 \in \{0,1\}$ by random,
$k = 0$, $\mathbf{t}^k = \mathbf{t}^0$ GOTO(7)
ELSE CO is terminated,

14: return $\mathbf{p}_0 = \mathbf{p}^*$;}
END *r*-th iteration;

15: Insert the new p_0 into **Algorithm 1: LM algorithm**.

To adjust small ergodic range around p_i^*, the parameters are set as $\gamma = 0.45$ [17], $\lambda = 4$ [18], $r_{\max} = 50$, and $K_{\max} = 50$. The value $\lambda = 4$ is set such that a significant difference in the long term will be obtained from a small change of t . As it can be seen from fig. 5 right, with a small change in two consecutive ***t***, a chaotic behavior will be observed in the time series manner (fig. 5 left). The value of $K_{\max}$ and $r_{\max}$ were chosen to minimize the overhead computational cost in determining the initial point. The statements IF $a_i^{r+1} > a_i^r$ THEN $a_i^{r+1} = a_i^r$, $\lambda \in \{0,0.5\}$ and IF $b_i^{r+1} < b_i^r$ THEN $b_i^{r+1} = b_i^r$, $\lambda \in \{0,0.5\}$ are to encourage movement farther from the initial bounding area, set in the beginning of the search. With reference to Fig. 4 (right), the initial guess is expected to lie on the correct optimization zone to find the global optimum.

6. Implementation and Discussion

6.1 Performance Improvement

Points with random error according to uniform distribution and normal distribution were generated as presented in table 1. For Chaos-LM method, initial point guess of the initial solution of LM optimization iteration was improved by sending it to CO method. In LM algorithm, the stopping rule is set as maximum iteration = 1000 and 100 for the Chaos-LM method. Fig. 6 visualizes the generated data by plotting the points cloud. The algorithm is implemented in MATLAB and run on an Intel Centrino Core 2 Duo 2.2 GHz.

Table 1: Details of data generation.

Type of Data		**Number of points and Nominal Parameter**		
		Circle	Sphere	Cylinder
Uniform	Range (μm)	*(x,y,r)*=(15,15,20) mm	*(x,y,z,r)*=(15,15,15,20) mm	(x,y,z,r)=(15,15,15,5) and ***n*** (1,1,1) mm
Type 1	[-2.2,2,2]	1000 pts	grid [30x30]	grid [25x25]
Type 2	[-5,5]	1000 pts	grid [30x30]	grid [25x25]
Normal	sigma σ			
Type 1	1.1	1000 pts	grid [30x30]	grid [25x25]
Type 2	2.5	1000 pts	grid [30x30]	grid [25x25]

The initial guess of the center of circle and sphere is the centroid. The centroid location for each *x,y,z* is the average of the points $\sum \mathbf{x}_i / n$. The centroid is also the initial guess of point on the axis of a cylinder. For the radius, its initial estimation is:

$$r_0 = \frac{1}{2}\left(\frac{(\max x_i - \min x_i) + (\max y_i - \min y_i)}{2}\right) \tag{8}$$

for the circle and:

$$r_0 = \frac{1}{2}\left(\frac{(\max x_i - \min x_i) + (\max y_i - \min y_i) + (\max z_i - \min z_i)}{3}\right) \tag{9}$$

for the sphere and cylinder. For the special case of a cylinder, its initial guess for cosine direction of the axis is derived by fitting a 3D line to the point clouds. The fitting method is implemented with a method according to NIST [6].Two levels of sigma for the data deviation were considered. Type 1 represents only the uncertainty of the instrument (Maximum Permissible Error/MPE), while type 2 simulates the uncertainty due to the part and the instrument. Type 2 data represents a more realistic situation since an inspected part always contains feature deviation from its nominal [19].

Results from 100 runs show that the combination of these methods, Chaos and LM, increases the accuracy of the fitting process. The indication is that the fitted geometry has less residual error, in term of the magnitude of their norm of sum of square residuals, while preserving the computation cost. Table 2 provides the complete results of the fitting of full geometry point clouds both with only LM method and with Chaos-LM method. Chaos-LM encourages the initial

guess of the solution to move to a better starting point, thanks to the property of the chaotic motion which non-repeatedly searches through a set of states in a certain bounded domain [15]. Sensitiveness of the final solution of LM method to where the initial guess starts is related to the Taylor approximation in the Gauss-Newton method, which depends highly on the non-linearity degree of the neighborhood. The quality of this Taylor approximation, which is usually until first term approximation, decreases for higher non-linear function. Because of this, a "trapped" condition during searching process can occur. Fig. 7, 8 and 9 propose some visualizations of the fitting result for circle, sphere and cylinder respectively. From this, one can observe that the Chaos-LM fitting (fig. 7, 8, and 9 right) finally lie on the middle of the point cloud. This is coherent with the fundamental behavior of least-square fitting which is an average over the considered data (in this case the point cloud). Plot of the norm of residual and Central Processing Unit (CPU) time for circle, sphere, and cylinder are respectively presented in fig. 10 and 11. In the special case of a cylinder fitting result, the computation time slightly increases compared to the LM method. Indeed, the improvement in the sum of squared residuals is significant. Furthermore, from the graph one can observe that the variation interval of the CPU time for this cylinder fitting is intersecting each other, so they are not significantly different.

Table 2: Simulation results of the full-geometric point cloud fitting.

	Levenberg-Marquardt Algorithm					
Random	Circle		Sphere		Cylinder	
Error Type [μm]	‖r‖ (μ±3σ) [mm]	CPU time (μ±3σ) [s]	‖r‖ (μ±3σ) [mm]	CPU time (μ±3σ) [s]	‖r‖ (μ±3σ) [mm]	CPU time (μ±3σ) [s]
U [-2.2,2.2]	75.2584±0.0627	0.8334±0.0502	4.1007±0.2632	1.0459±0.1059	71.427±0.0646	0.5114±0.0512
U [-5,5]	75.26±0.0548	0.8081±0.0244	7.6507±1.2160	0.5935±0.0442	71.4316±0.1288	0.6317±0.0825
N (σ=1.1)	75.2265±0.0166	0.825± 0.0376	1.5108±0.0202	1.0353±0.1272	71.4232±0.0150	0.6368±0.0766
N (σ=2.5)	75.225±0.0375	0.8754±0.1270	1.6651±0.0453	1.0694±0.1653	71.4252±0.0363	0.6276±0.0804
	Chaos and Levenberg-Marquardt Algorithm					
Random	Circle		Sphere		Cylinder	
Error Type [μm]	‖r‖ (μ±3σ) [mm]	CPU time (μ±3σ) [s]	‖r‖ (μ±3σ) [mm]	CPU time (μ±3σ) [s]	‖r‖ (μ±3σ) [mm]	CPU time (μ±3σ) [s]
U [-2.2,2.2]	5.6646±1.6784	0.5578±0.0539	2.79±0.2570	0.5634±0.05555	5.7257±2.0102	0.6225±0.0277
U [-5,5]	4.3562±1.3061	0.5551±0.0338	6.2199±0.4602	0.5628±0.1088	5.7994±2.9641	0.6706±0.0515
N (σ=1.1)	5.1907±1.2732	0.5677±0.1053	0.4279±0.1524	0.5458±0.0569	6.9329±2.9690	0.6788±0.0907
N (σ=2.5)	5.469±1.4621	0.5442±0.0836	0.8185±0.0991	0.4663±0.0512	6.9169±1.6543	0.6987±0.1103

A very important condition, difficult to address with standard approaches to fitting, arises when the cloud of points does not cover the whole feature, e.g. only a hemisphere has been sampled. This may be due to access limitation of the sensor to capture part surface, like e.g. in the case of laser scanning instruments, or to the real incompleteness of the sphere, like in the case of a circular groove. Both LM and Chaos-LM methods are applied to half-circle, half-sphere, and half-cylinder point clouds. This is a significantly more difficult situation compared to fitting a complete cloud of points. One of the reasons is that the estimation of initial solution tends to be

less accurate since, in general, the initial estimation is based on the symmetrical properties of the geometry to be fitted. The data generation is identical to the one considered for the full-geometry case as presented in table 1. From this data generation, half of the cloud of points is then discarded to get the half-geometry. The number of runs in the simulation and the performance measures of both fitting methods are identical to the previous "normal case". Details of all results of the simulation runs are presented in table 3. One can observe that the accuracy of fitting half-geometry point clouds is significantly improved by Chaos-LM method compared to only LM method. Instead, the CPU time needed for Chaos-LM to have better result is higher than the one of the LM method. Since there are increments in CPU time to get a better result of Chaos-LM method, the comparison of the two algorithms in this case has to be further investigated. Graphical presentation of the fitting results for half-circle, half-sphere and half-cylinder are provided in fig. 12, fig.13, and fig. 14 respectively to intuitively understand the significant result of accuracy improvement by Chaos-LM in the case of half-geometries fitting. Finally, to graphically explain the results in table 3, fig. 15 and fig. 16 respectively plot the norm of residual $\|r\|$ and CPU time of the half-geometries fitting.

Table 3: Simulation results of the half-geometric point cloud fitting.

Random Error Type [μm]	**Levenberg-Marquardt Algorithm**					
	Circle		Sphere		Cylinder	
	‖r‖ (μ±3σ) [mm]	CPU time (μ±3σ) [s]	‖r‖ (μ±3σ) [mm]	CPU time (μ±3σ) [s]	‖r‖ (μ±3σ) [mm]	CPU time (μ±3σ) [s]
U [-2.2,2.2]	88.0124±0.0087	0.8263±0.0610	41.9479±0.4454	0.2918±0.0128	41.2638±0.0271	0.6307±0.0412
U [-5,5]	88.0106±0.0209	0.8364±0.0869	41.1334±0.9747	0.2931±0.0153	41.2651±0.0510	0.6273±0.0557
N (σ=1.1)	88.0143±0.0021	0.4542±0.0535	21.2072±0.0603	0.2916±0.0155	41.2643±0.0067	0.4978±0.0159
N (σ=2.5)	88.0149±0.0053	0.4634±0.0551	21.1117±0.1741	0.2957±0.0285	41.2636±0.0140	0.6243±0.0895
Random Error Type [μm]	**Chaos and Levenberg-Marquardt Algorithm**					
	Circle		Sphere		Cylinder	
	‖r‖ (μ±3σ) [mm]	CPU time (μ±3σ) [s]	‖r‖ (μ±3σ) [mm]	CPU time (μ±3σ) [s]	‖r‖ (μ±3σ) [mm]	CPU time (μ±3σ) [s]
U [-2.2,2.2]	14.8104±7.5609	1.2904±0.0361	8.5878±4.8903	0.5509±0.0450	18.9191±3.1847	1.2009±0.0611
U [-5,5]	15.9923±12.0558	1.2212±0.1456	9.2163±6.3610	0.413±0.0247	18.7634±3.0584	1.2185±0.1001
N (σ=1.1)	15.0230±13.5643	1.2944±0.0831	4.9317±4.002	0.4170±0.0269	18.7751±3.5261	1.0946±0.1623
N (σ=2.5)	16.7502 ±12.1930	1.3000±0.08	4.9572±2.3395	0.55±0.0335	19.1193±4.0786	1.2163±0.0627

Convergence curve analyses are presented in two parts which are for full- and half- geometries fitting. One should note that in both cases, the value of convergence curve can not reach zero since error exist on the points to be fit due to the simulated perturbation. The selected type of simulation is uniform distribution in the range of -5μm and 5 μm **U** [-5,5]. For each group, three convergence curves are shown corresponding to circle, sphere and cylinder. On the x-axe of the graph, there are two types of iteration. For LM method, it corresponds to LM number of iterations which ranges from 100 to 1000 iterations. For Chaos-LM, this axis corresponds to the number of chaos iteration in the range from 10 to 100 iterations. In the case of full-geometric fitting, the convergence rate is much faster in the case of circle and cylinder. Fig. 17, fig. 18, and fig. 19 depict the convergence curves for the full-geometries case. The convergences rate of LM method for circle and cylinder fitting are much slower, as the small gradient of the curve compared to the Chaos-LM one denotes. In the case of the sphere, both LM and Chaos-LM method have a similar convergence rate though Chaos-LM method is faster with respect to the LM one. Clearer "trapped" phenomena of LM method in fitting can be observed in the case of half-geometries fitting problem. The convergence curves for the half-geometries are shown in fig. 20, fig. 21, fig. 22 respectively. From all these three figures, the LM method does not show improvement as the number of LM iterations is increased. This situation clearly shows that LM has been trapped in some local optimum region. It means that, although the number of iteration is increased, the result of LM can not give a better result so one can say it is "early converged". On the other hand, a different situation can be seen for the Chaos-LM method. This method can escape from a local optimum with an increase of the chaos iterations. The reason is that, by using chaotic movement and increasing the number of iterations, more regions are visited to explore new better feasible solution that can give a better result. Chaos-LM can show a significant improvement and convergence result without a large number of iteration increments. From the investigation of the convergence, one can observe that the best number of chaos iterations for Chaos-LM is around 30.

The chaos optimization to improve the initial guess is effective in LS fitting problem. The chaos search encourages the initial guess of the solution to move to a better starting point that is nearer to the true solution thanks to the property of the chaotic motion that non-repeatedly searches through a set of states in a certain bounded domain [20]. With this property, the searching process can cover a wider search space within a small number of iteration. This is a different property compared to improvement heuristic search such as genetic algorithm, tabu search, etc [21]. Generally, improvement heuristic searches algorithm need larger number of iterations to increase the "visited feasible solution" around the search space in which the computational cost becomes problematic.

Combinations of Chaos and LM algorithms have a linear complexity in term of the relation between number of points processed and the increase in computation time. One can see that they are constructed from two algorithms, which are the Chaos and the LM algorithm. Each of them contains two nested loops inside their algorithm. Since the two loops of the algorithm are not related to the number of the points *n*, which are the points to be fitted, the relation of the algorithm steps to their inputs is only in the calculation to evaluate the objective function through all number of points n. Let the total order of the algorithms be $f(n) = n_1 + n_2 = n + n = 2n$ where subscript 1 and 2 correspond to algorithm 1 (chaos) and 2 (LM), respectively. Hence, the

algorithm efficiency is $O(n)$ since $\exists n_0 > 0 \ and \ k > 0 \Rightarrow \forall n > n_0, f(n) \leq k.g(n)$ such that $f(n) = n_1 + n_2 = O(n)$.

6.2 Case Studies

To test the Chaos-LM method in a real fitting situation, a case study was carried out. It is derived from Kawalec and Magdziag [22]. In their case, a calibrated ring gauge was used since they focused on comparison of methods to solve the circle fitting problem. Instead, in the proposed case study, measurement of a calibrated ceramic sphere of a "ZEISS" CMM for stylus qualification was used as shown in fig. 23. The sphere has a calibrated radius of 14.991 mm. The CMM machine used was "ZEISS PRISMO HTG" with MPE_E=2 μm+L/300 μm. The choice of sphere is due to the fact that a 3D geometry fitting can be applied and a sphere is a good example of a common artifact for CMMs. The strategy used to obtain the points was by means of scanning strategy. The point cloud to be fit is a half-geometry. There are two types of point clouds. The first type is low density cloud and the second type is high density (fig. 24). The low density point cloud contains 312 points. A total of 3435 points were collected for high density point cloud. The initial parameter of the sphere, for both LM and Chaos-LM method, has been chosen near the optimal. The initial x and y are from the average of respectively x- and y-position of the points, and z is selected from maximum z-position of the points minus the known nominal radius of 15 mm. Table 5 summarizes both the fitting results and the deviation from the calibrated radius of the sphere. From the results, the fitted radius of the sphere from Chaos-LM method is much better than the LM one. Note that the results of LM method are already from 50000 iterations. Both in the low and high density cases, the procedures are run with the same number of iteration. In the case of low density, the accuracy is even better than in the high density one since for high density, more solution space is obtained such that an increase of iterations can produce similar results with regard to the lower density result. Visualization of the fitting results is provided in fig. 25 both for low and high density points respectively.

Another case study was carried out by measuring and fitting an industrial-made cylinder work piece made of hardened steel having nominal diameter of 6 mm. The measurement procedure is shown in fig. 26a. Total points obtained were 190 points by circular path scanning strategy of three segments. Fig. 26b presents the fitting result. The blue points are the obtained points. Meanwhile, the red points are the fitted cylinder with its axis line in green. Since the geometry is symmetry, the selection for initial parameters is identical to the one set in the simulation run of section 6.1 for cylinder case. The results show the improvement of Chaos-LM fitting. Details of the results are depicted in table 6. The cylinder is not calibrated. Subsequently, the norm of residual $\|r\|$ is presented to compare the fitting quality. In this case, Chaos-LM gives better result. Moreover, from the table, it can be observed that the fitting result by LM is outside the tolerance limit, meanwhile the Chaos-LM result is inside.

Table 5: Results of fitting half-calibrated sphere for high and low density point cloud.

	x (mm)	y (mm)	z (mm)	radius (mm)	deviation from calibrated radius (mm)
Calibrated Value	-	-	-	14.9911	-

High Density					
LM Method	68.2182	-66.1638	41.9932	14.9111	0.08001
Chaos-LM Method	67.5716	-66.7949	42.2488	14.9919	0.00080
Low Density					
LM Method	68.261	-66.1605	41.9712	14.9009	0.09020
Chaos-LM Method	67.5458	-66.7681	42.2524	14.9904	0.00070

Table 6: Results of fitting industrial cylinder.

	x [mm]	y [mm]	z [mm]	nx	ny	nz	Diameter [mm]	|| r || [mm]
Nominal Value	-	-	-				6 ± 0.01	
LM Method	39.7946	37.5621	39.6751	-0.007	-0.0181	-0.9191	5.928	3.489
Chaos-LM Method	39.6788	37.2259	38.9024	-0.0531	-0.0571	-1.8548	6.0018	1.8278

7. Concluding Remarks

The problem of fitting non-liner geometries has been addressed. This problem is critical in dimensional metrology to assure the quality of manufacturing products. The geometries considered are circle, sphere and cylinder due to their various and common use in applications such as metrological calibration and mechanical assembly. The increasing capability of modern metrology instruments in sampling high density clouds of points in short time demands accurate and fast fitting procedures. Both cases of fitting full- and half-geometries are presented. From the fitting of full-geometries, results show that the use of chaos optimization to improve the initial guess for LM non-linear least square fitting has significantly improved the accuracy of the fitting and kept the computational time small. A slower fitting is observed in the case of half-geometries. Even though slower, Chaos-LM method can give the expected results by escaping from local optima. LM method is trapped and early converged in the case of half-geometries fitting, so that no improvement of the result can be obtained by increasing the number of iterations. Convergent rate efficiency of the proposed method is significantly higher in the case of incomplete points cloud. It seems that the LM method could have higher probability to be trapped in the local optima in this case. Two real case studies are presented. The case studies are to fit a calibrated sphere from point clouds representing half of the sphere geometry and to fit an industrial-made cylinder. The Chaos-LM method gives expected results. Finally, a note should be highlighted that a filtering procedure of the point cloud may be needed before the fitting process is carried out, since least-square fitting procedure is not completely robust to the outlier points. The future direction of this work is to identify the link between the non-linear problem and chaos property such that an adaptive region bounding and chaotic motion generation can be determined precisely.

Acknowledgements

Financial support to this work has been provided as part of the project REMS - Rete Lombarda di Eccellenza per la Meccanica Strumentale e Laboratorio Esteso, funded by Lombardy Region (Italy), CUP: D81J10000220005.

References

[1] Loch C H, Van der Heyden L, Van Wassenhove L N, Huchzermeier A, Escalle C, 1999, Industrial excellence: management quality in manufacturing, Springer: London.

[2] Kunzmann H, Pfeifer T, Schmitt R, Schwenke H, Weckenmann A 2005 Productive Metrology-Adding Value to Manufacture *CIRP Ann. Manuf. Techn.* 54(2) 155 – 168.

[3] Pereira P H 2012 Cartesian Coordinate Measuring Machines, in Hocken R. J., Pereira, P. H (Eds), Coordinate Measuring Machines and Systems 2nd ed, (Florida:CRC Press) 57-79.

[4] Morse E 2012 Operating a Coordinate Measuring Machine, in Hocken R. J., Pereira, P. H (Eds), Coordinate Measuring Machines and Systems 2nd ed, (Florida:CRC Press) 81-91.

[5] Wilhelm R G, Hocken R, Schwenke H 2001 Task Specific Uncertainty in Coordinate Measurement *CIRP Ann. Manuf. Techn.* 50(2) 553-563.

[6] Shakarji C M 1998 Least-Squares Fitting Algorithms of the NIST Algorithm Testing System, *Journal of Research NIST* 103 633-641.

[7] Hoppe H, DeRose T, Duchamp T, McDonald J, Stuetzle W 1992 Surface reconstruction from unorganized points *ACM* 26(2) 71-78.

[8] Moroni G, Petrò S, Tolio T 2011 Early cost estimation for tolerance verification *CIRP Ann. Manuf. Techn.* 60(1) 195-198.

[9] ISO 10360-4:2010 2010 Acceptance and re-verification test for coordinate measuring machines: CMM used in scanning measuring mode.

[10] ISO 10360-5:2010 2010 Acceptance and re-verification test for coordinate measuring machines: CMM using single and multiple styluses contacting probing system.

[11] Whitney D E 2004 Mechanical Assemblies: Their Design, Manufacture, and Role in Product Development (USA: Oxford University Press).

[12] Marquardt D W 1963 An Algorithm for Least-Squares Estimation of Non-linear Parameters, *J. Soc. Ind. Appl. Math.* 11(2) 431-441.

[13] Nash J C 1979 Compact Numerical Methods for Computers Linear Algebra and Function Minimization (Bristol: Adam Higler Ltd).

[14] Rardin R L 2006 Optimization in Operation Research (New York: Addison-Wesley).

[15] Syam W P and Al-Harkan I M 2010 Comparison of Three Meta Heuristics to Optimize Hybrid Flow Shop Scheduling Problem with Parallel Machines, *World Academy of Science, Engineering and Technology* 62 271-278.

[16] Luo Y Z, Tang G J, Zhou N L 2008 Hybrid approach for solving systems of nonlinear equations using chaos optimization and quasi-Newton method *Applied Soft Computing* 8(2) 1068-1073.

[17] Tavazoei M S and Haeri M 2007 An optimization algorithm based on chaotic behavior and fractal nature *Comput. Appl. Math.* 206(2) 1070-1081.

[18] Yang D, Li G, Cheng G 2009 On the efficiency of chaos optimization algorithms for global optimization *Chaos, Solitons & Fractals* 34(4) 1366-1375.

[19] Kruth J P, Van Gestel N, Bleys P, Welkenhuyzen F. 2009 Uncertainty determination for CMMs by Monte Carlo simulation integrating feature form deviations *CIRP Ann. Manuf. Techn.* 58(1) 463-466.

[20] Jiang B L W 1998 Optimizing complex functions by chaos search. *Cybern. Syst*. 29(4) 409-419.

[21] Trafalis T B and Kasap S 2002 A novel metaheuristic approach for continuous global optimization *J. Global. Optim*. 23 171-190.

[22] Kawalec A and Magdziak M 2012 Usability assessment of selected method of optimization for some measurement task in coordinate measurement technique *Measurement* 45 2330-2338.

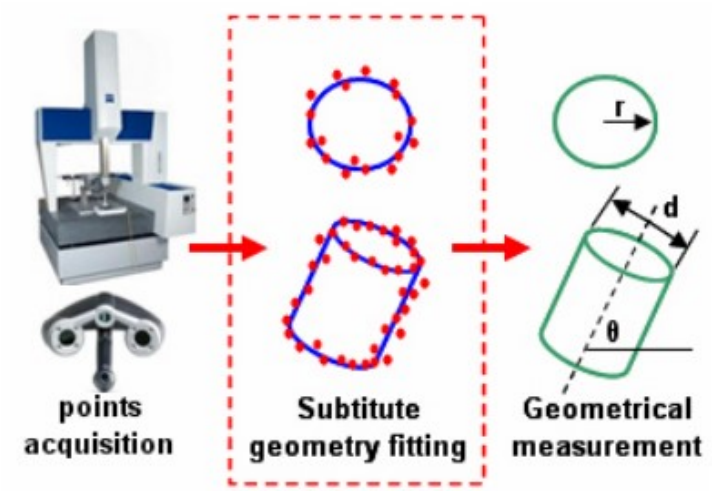

Figure 1: Critical step of geometrical fitting process in metrology.

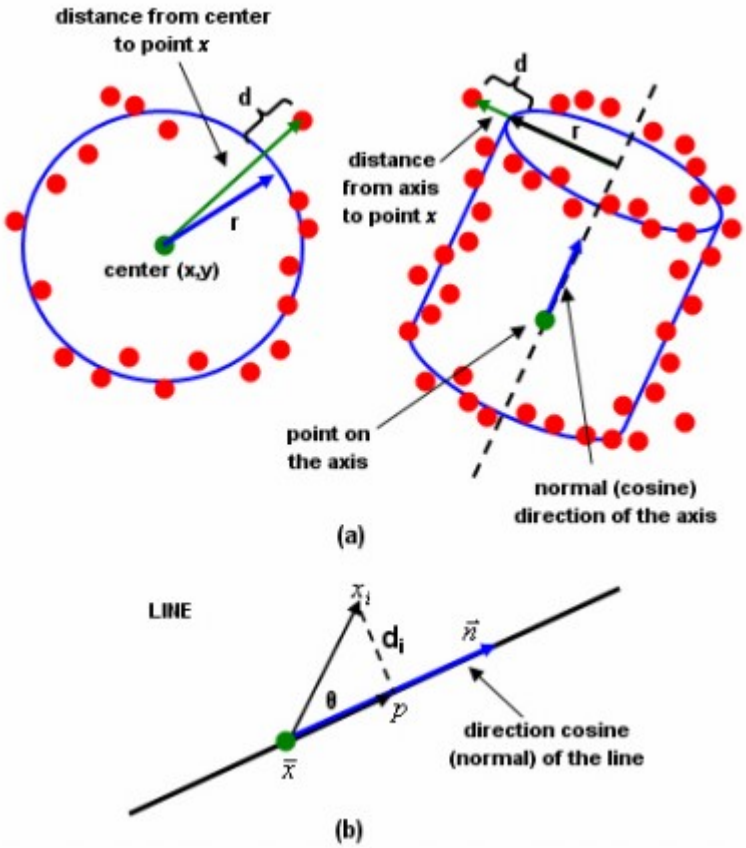

Figure 2: (a) Definition of point distance for circle (sphere) and cylinder, (b) Definition of point distance for 3D-line.

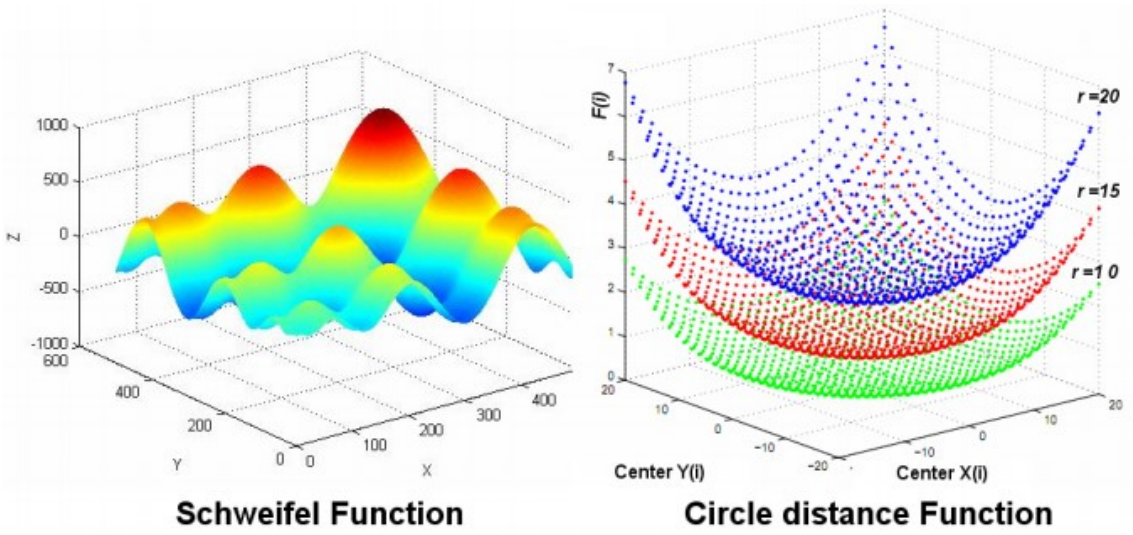

Figure 3: Illustration of Schweifel and Square of circle distance multimodal function.

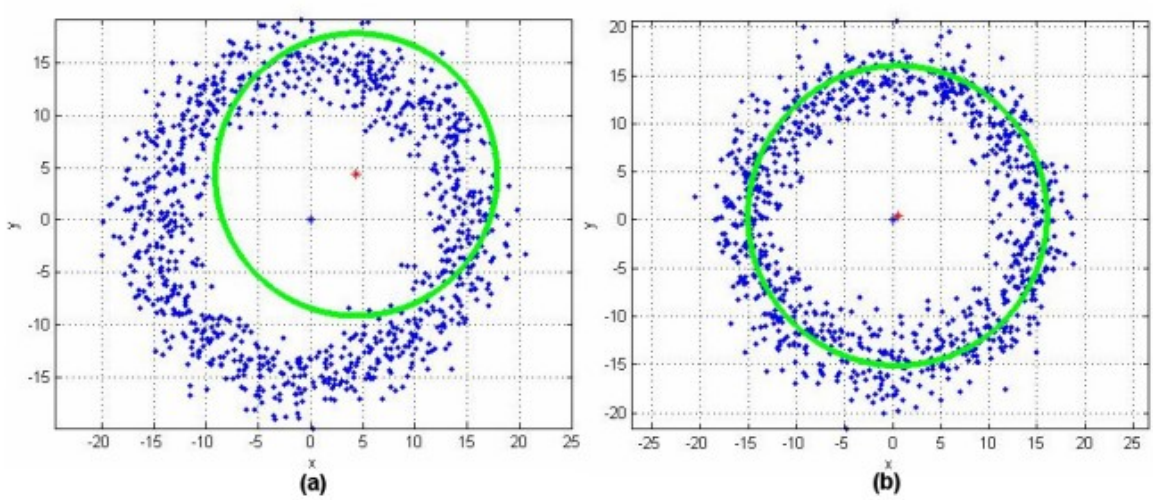

Figure 4: Different initial solutions affect the final solution. (a) Initial guess is far from optimal, (b) initial guess is near optimal.

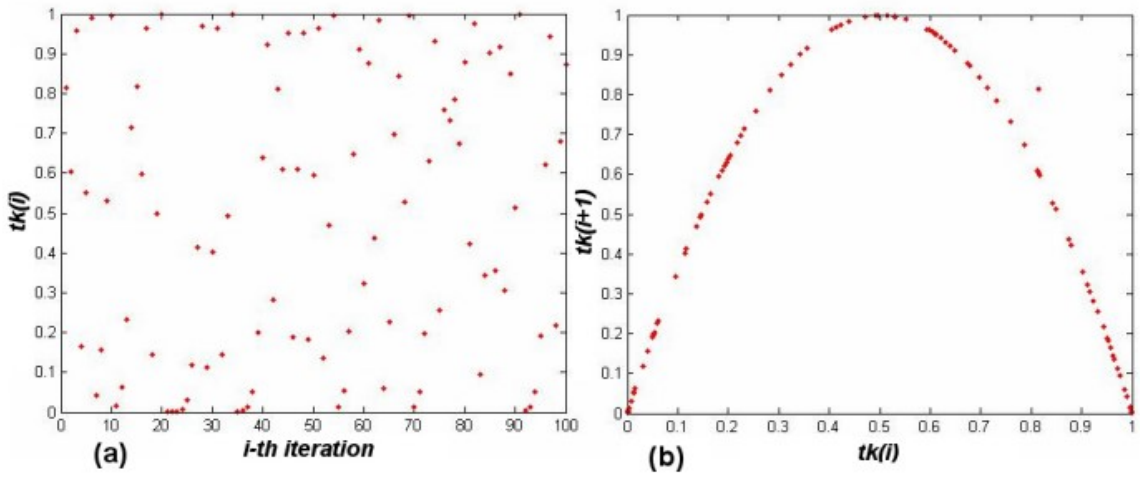

Figure 5: Logistic map. (a) time-series plot of logistic map, (b) paired-plot between two consecutive chaos variables.

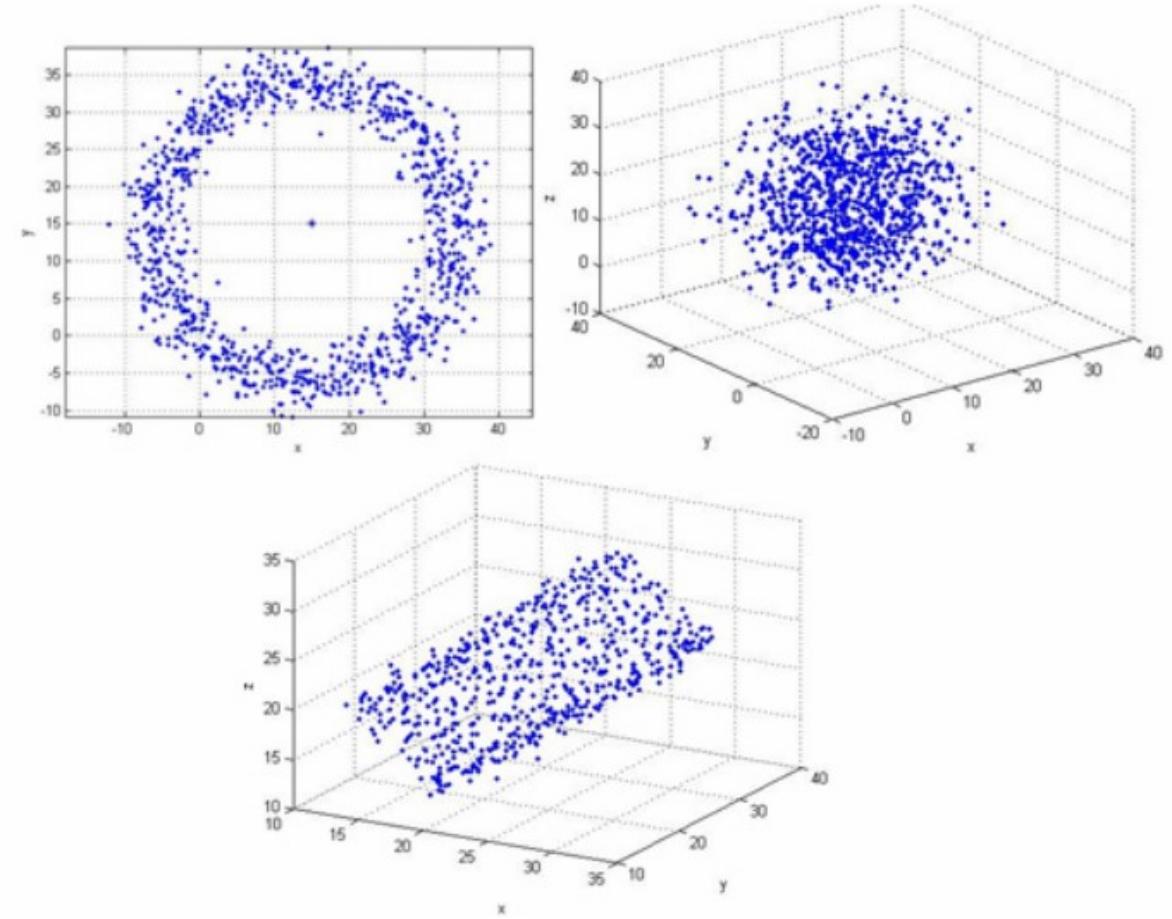

Figure 6: Illustration of data generated for circle, sphere, and cylinder.

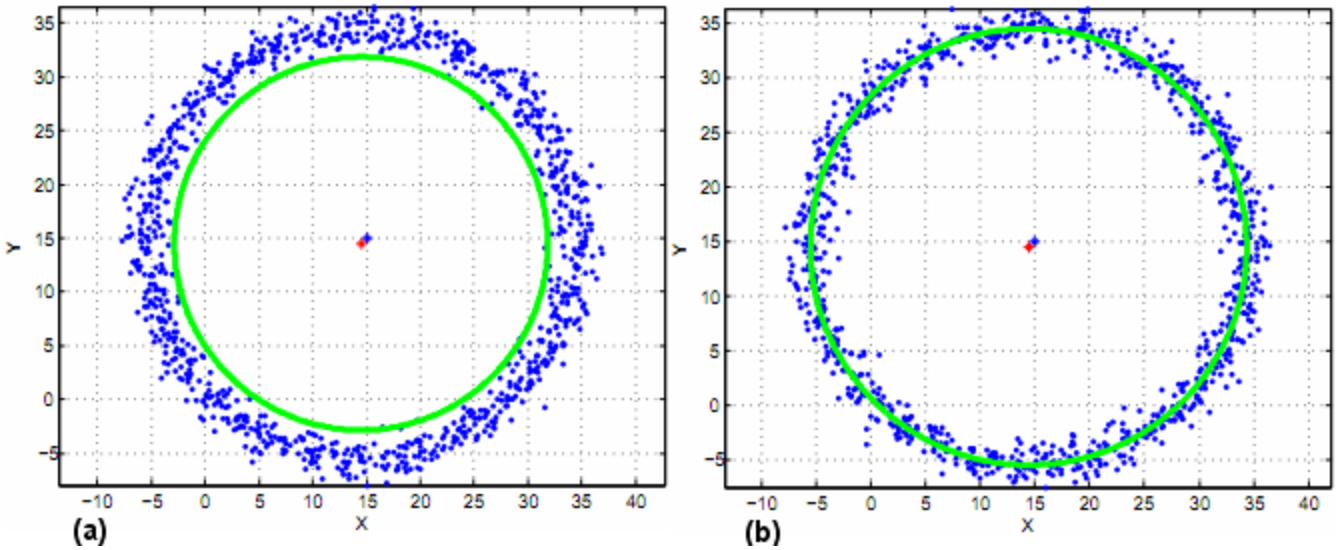

Figure 7: Substitute full circle fitting results of (a) LM method and (b) Chaos-LM.

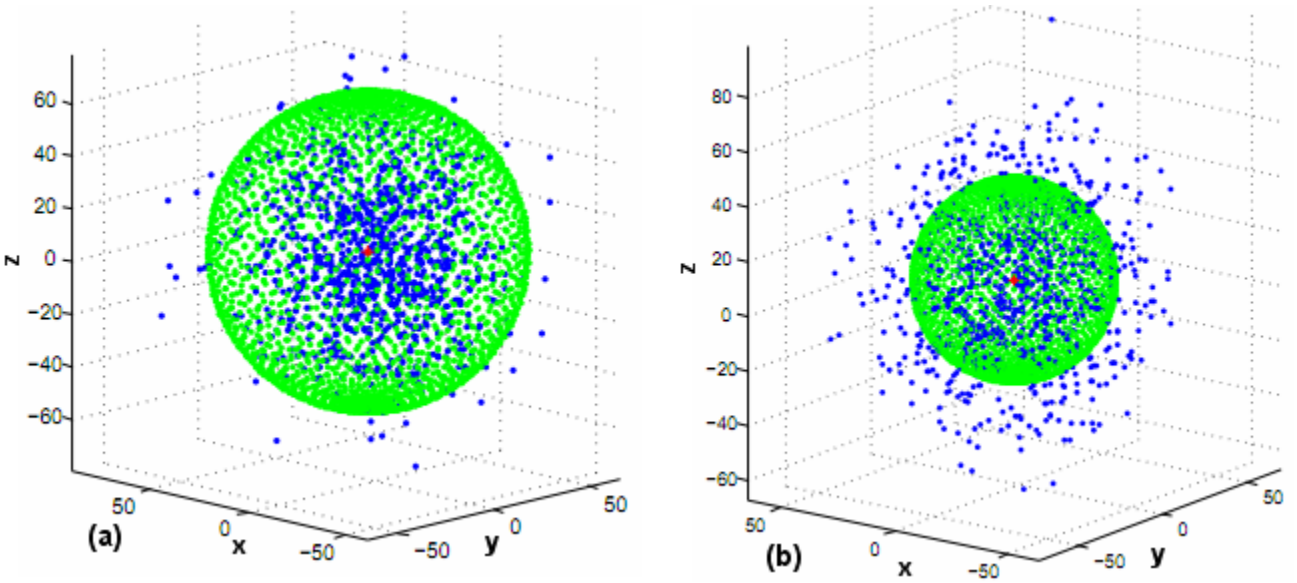

Figure 8: Substitute full sphere fitting results of (a) LM method and (b) Chaos-LM.

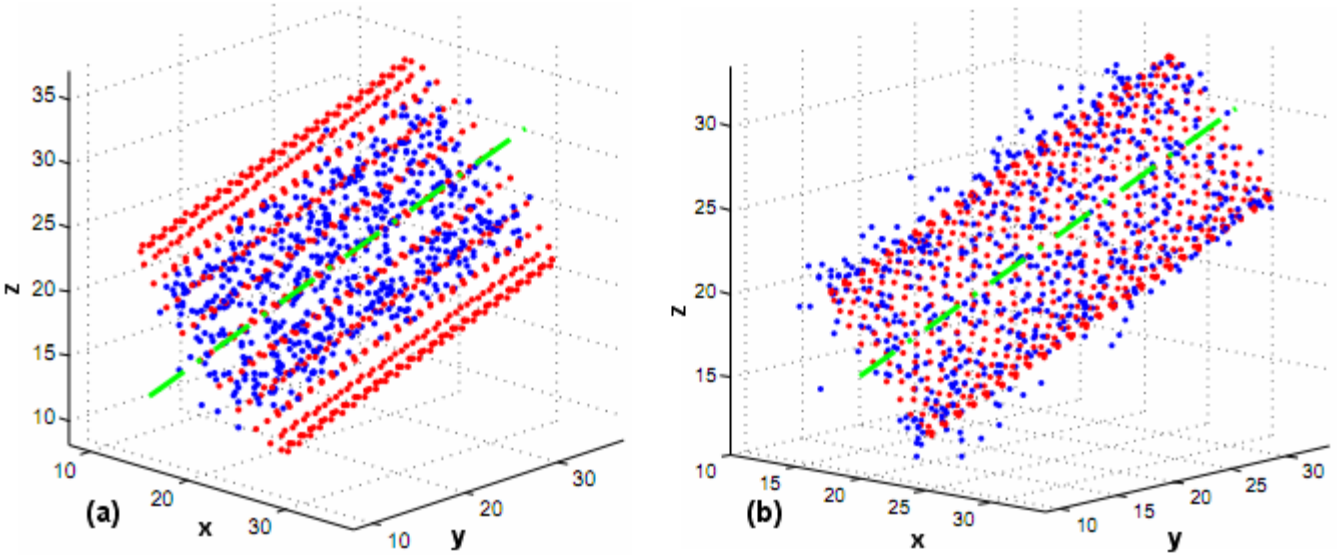

Figure 9: Substitute full cylinder fitting results of (a) LM method and (b) Chaos-LM.

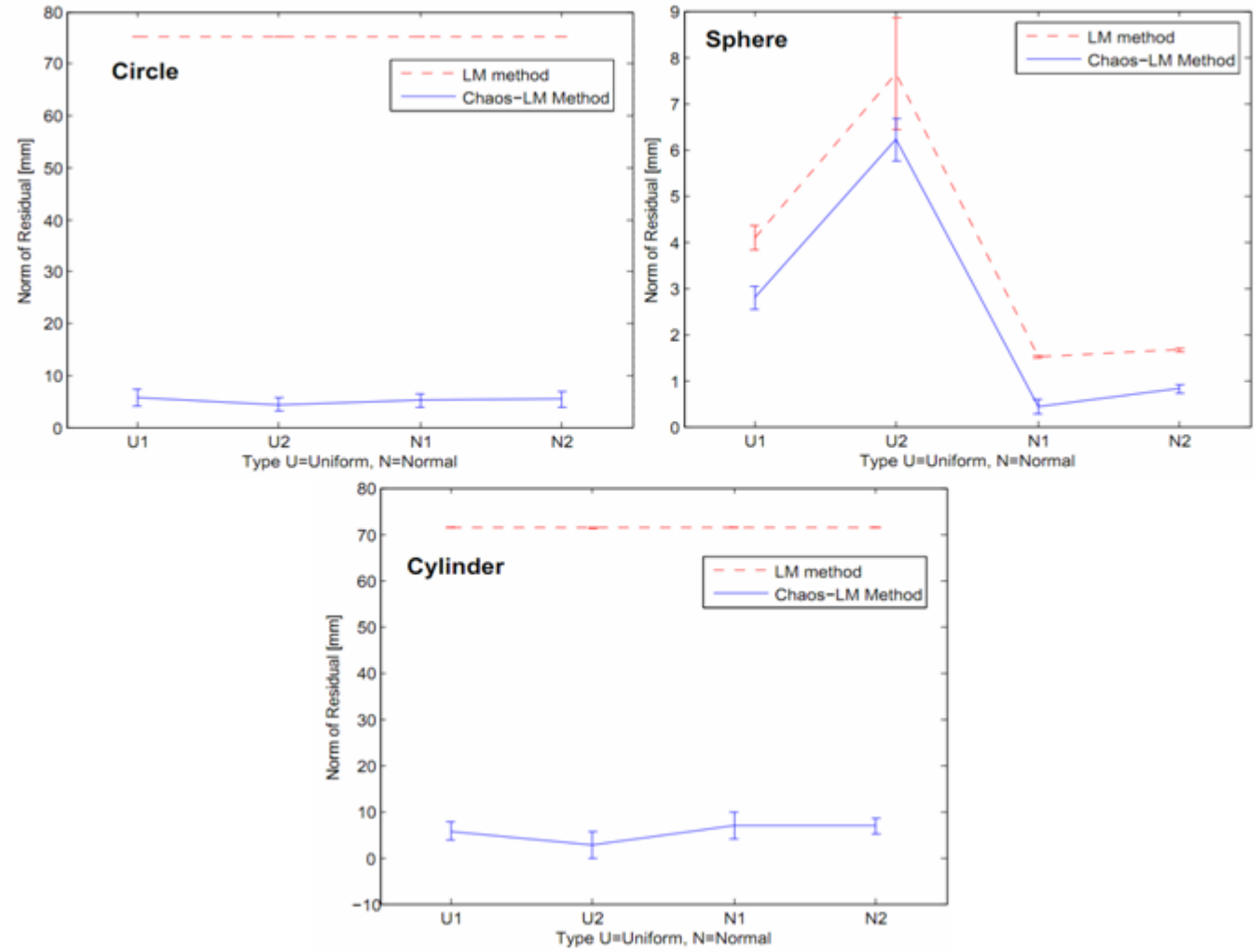

Figure 10: Norm of residual of LM method and Chaos-LM method for full point cloud geometry fitting.

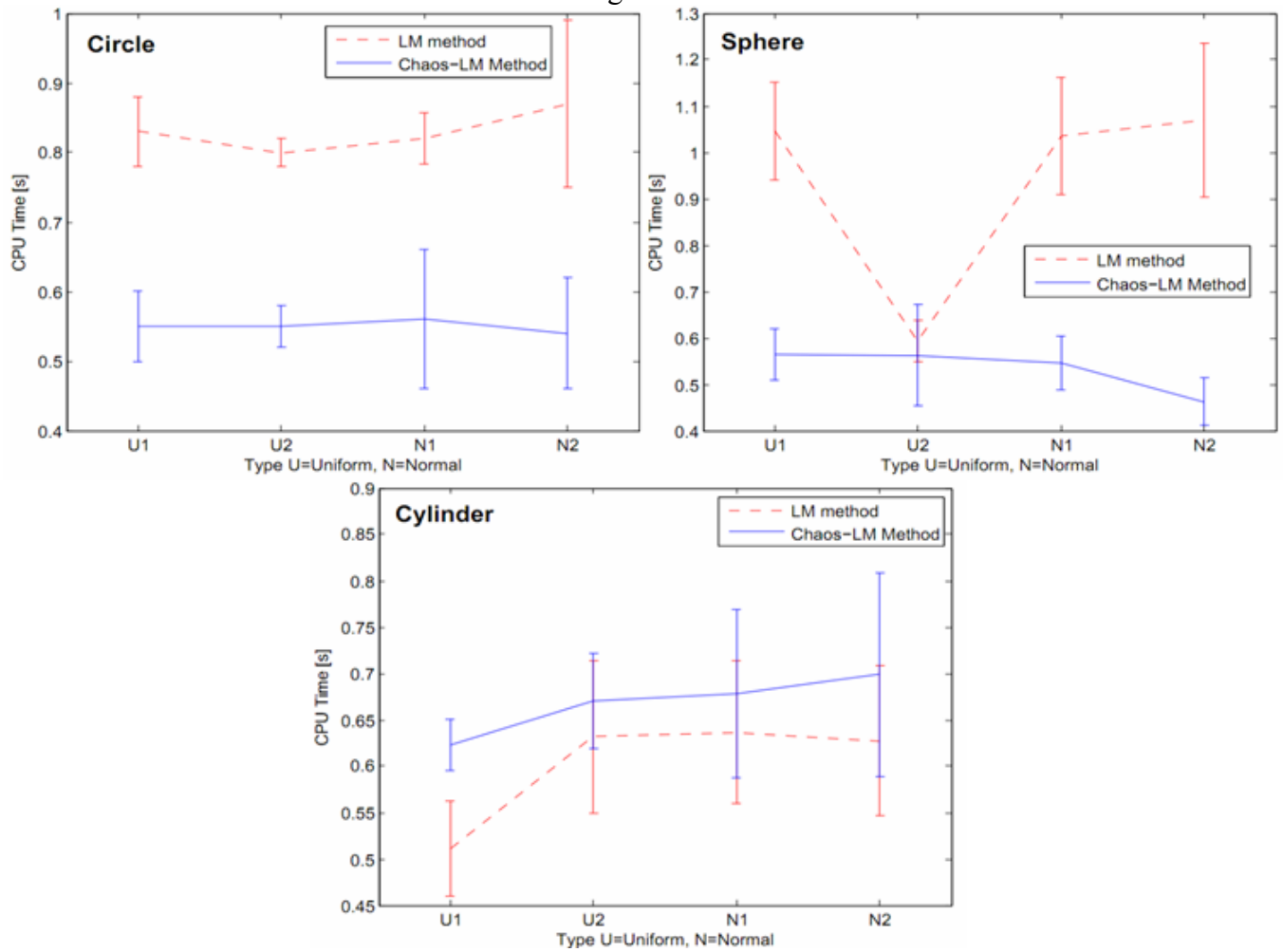

Figure 11: CPU time of LM method and Chaos-LM method for full point cloud geometry fitting.

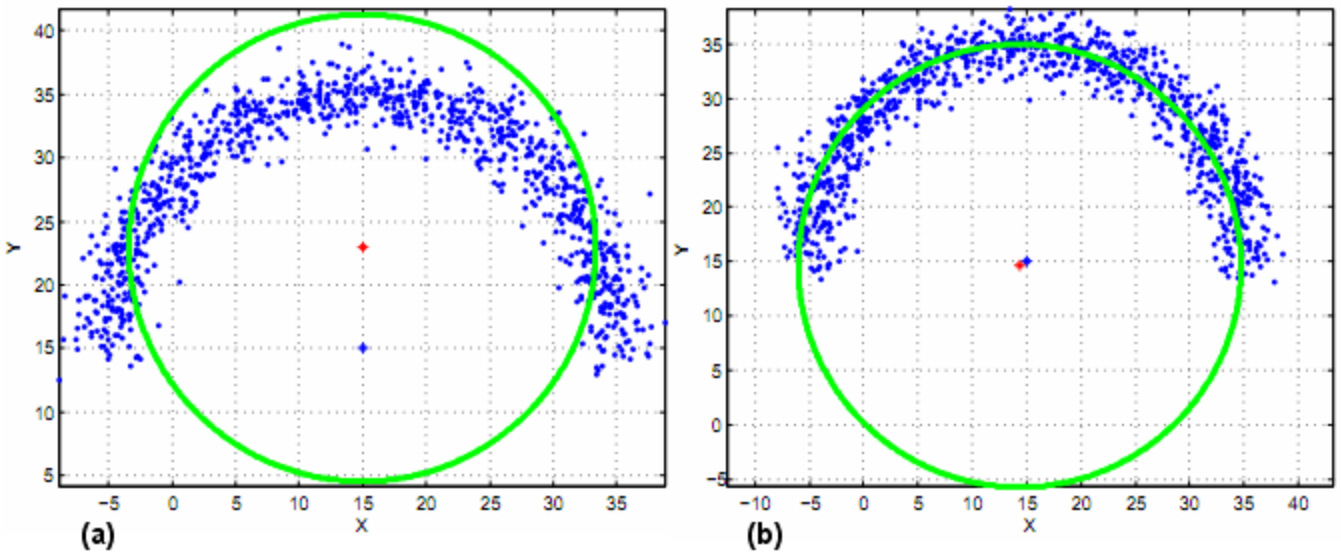

Figure 12: Substitute Half circle point cloud fitting results of (a) LM method and (b) Chaos-LM.

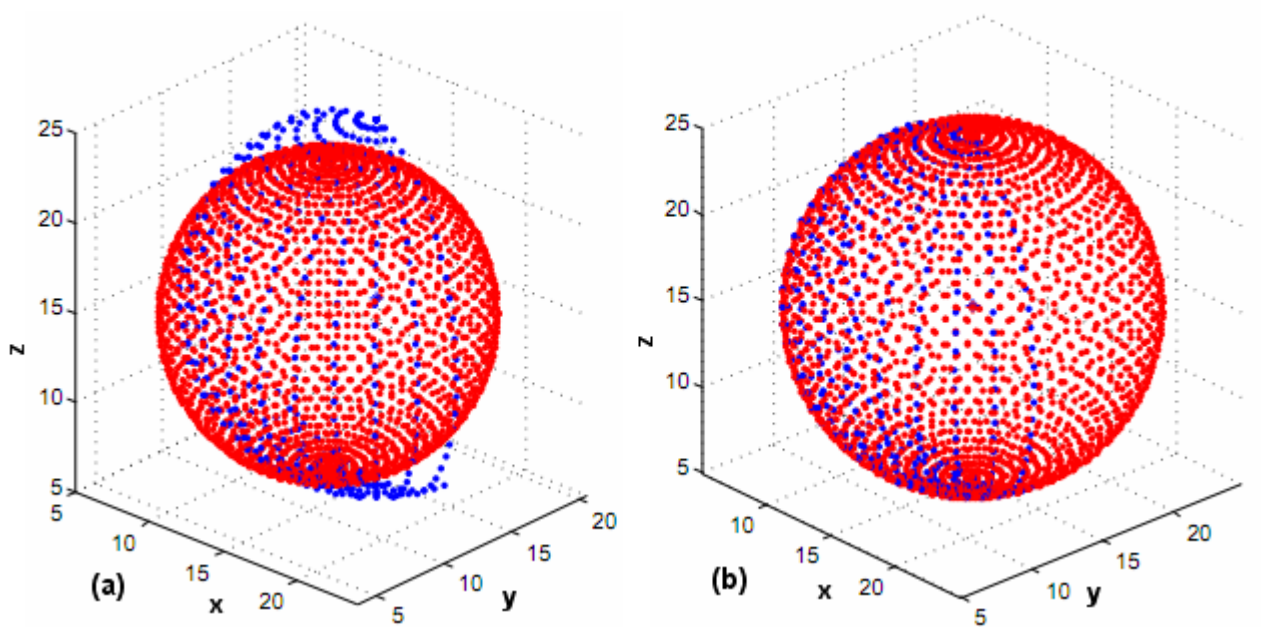

Figure 13: Substitute Half sphere point cloud fitting results of (a) LM method and (b) Chaos-LM.

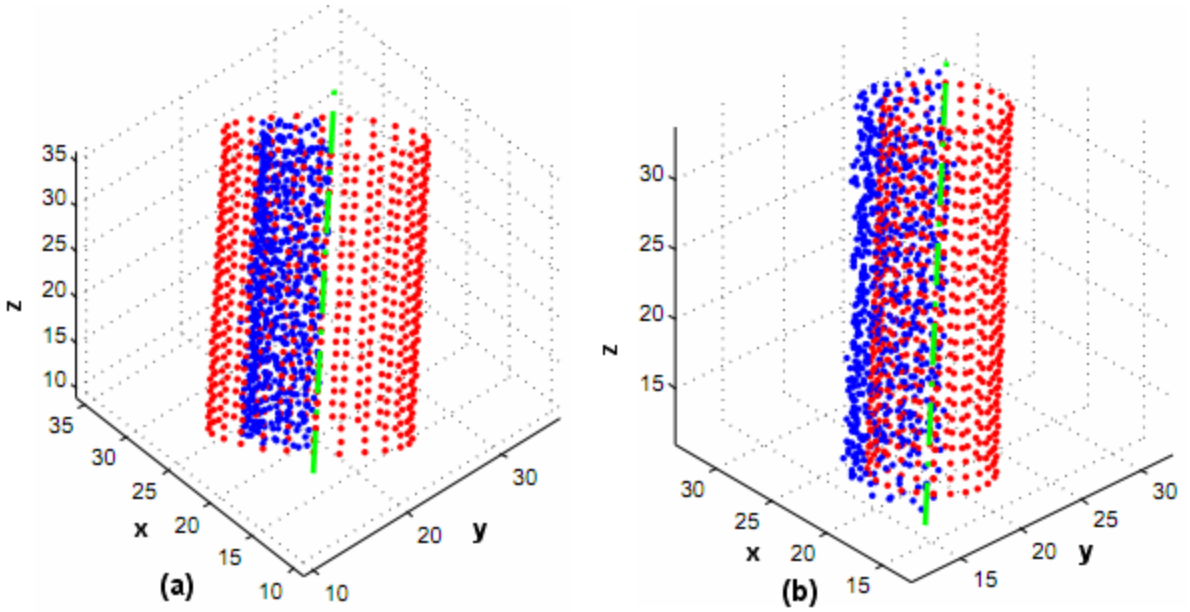

Figure 14: Substitute Half cylinder point cloud fitting results of (a) LM method and (b) Chaos-LM.

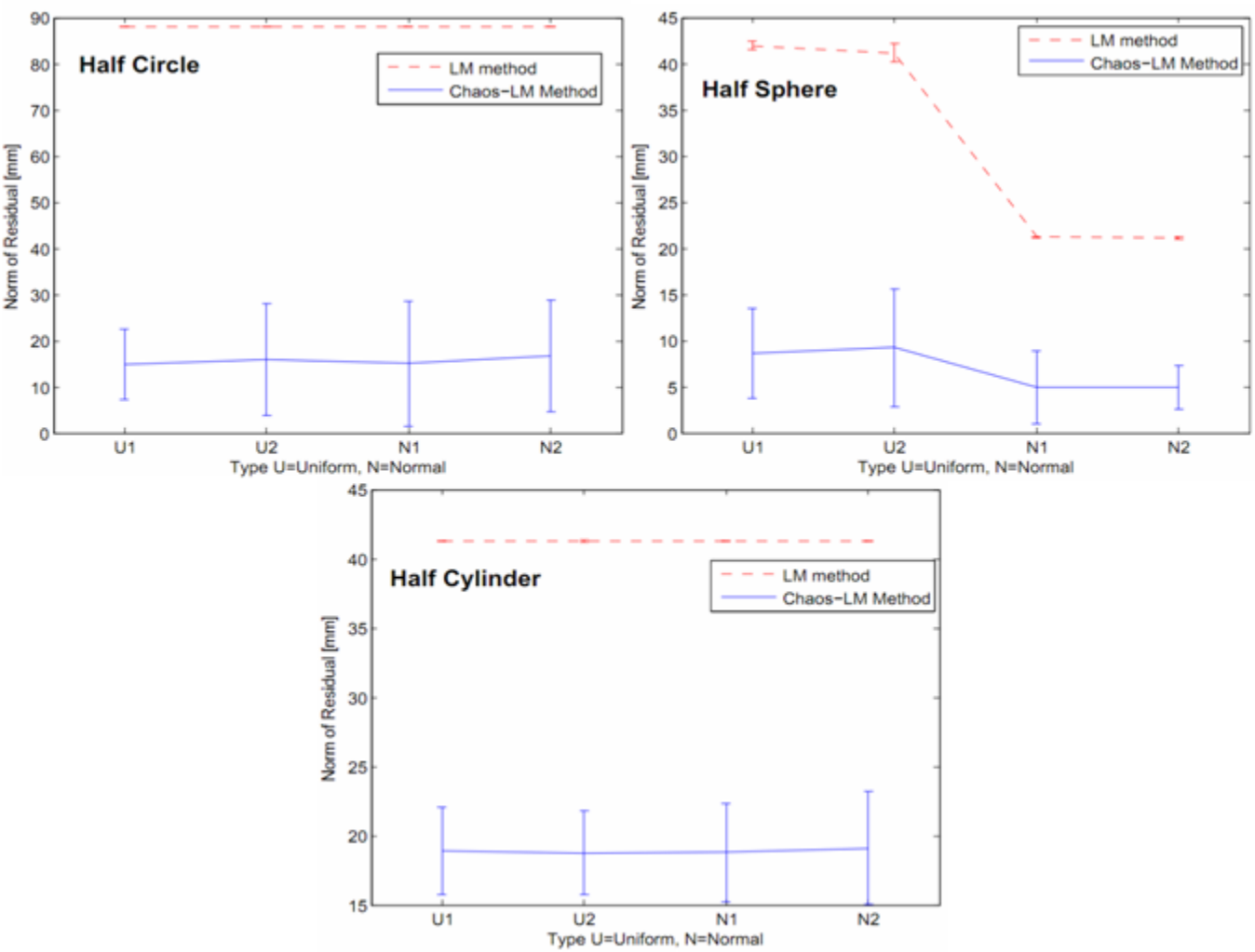

Figure 15: Norm of residual of LM method and Chaos-LM method for Half point cloud geometry fitting.

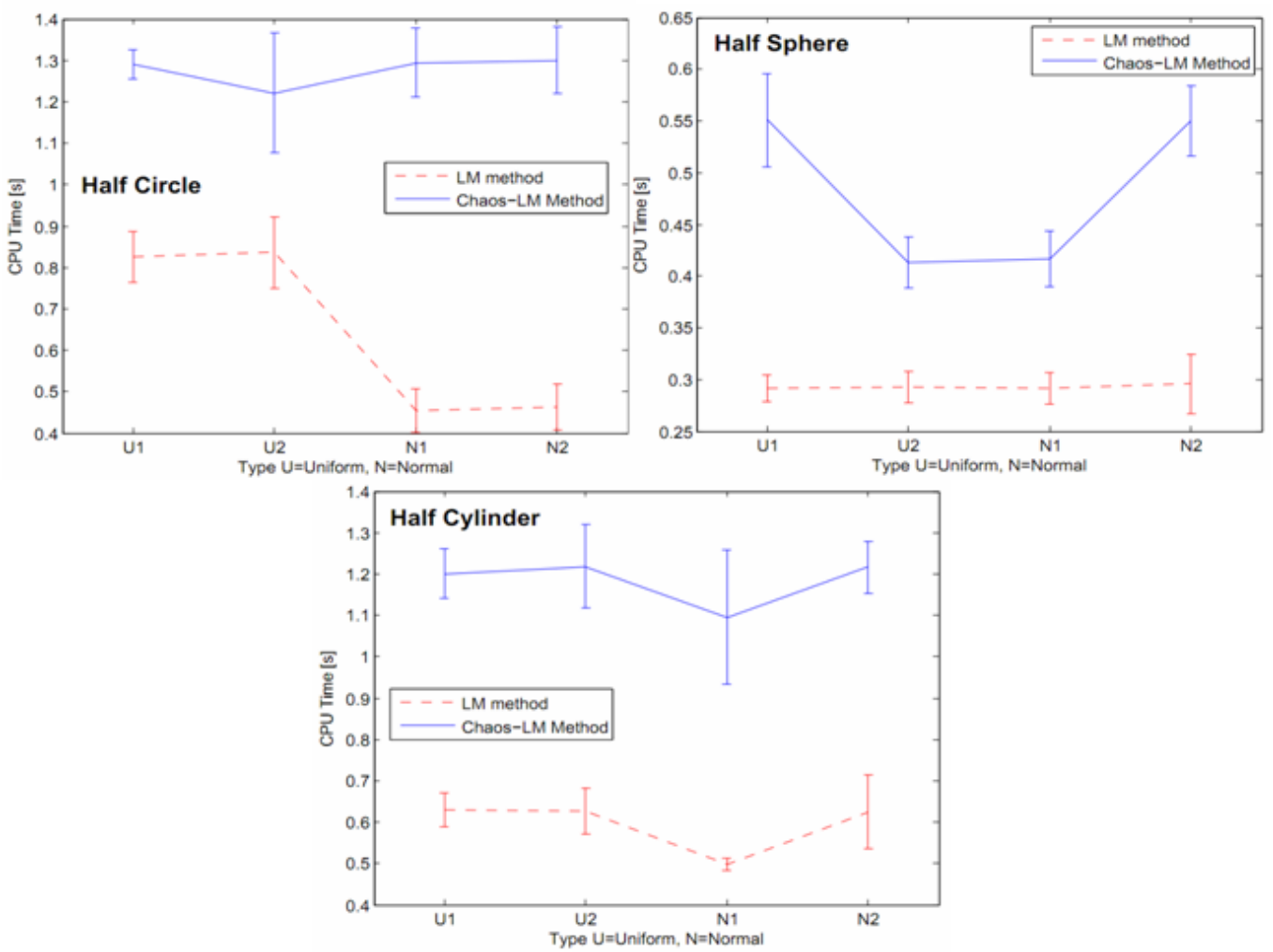

Figure 16: CPU time of LM method and Chaos-LM method for Half point cloud geometry fitting.

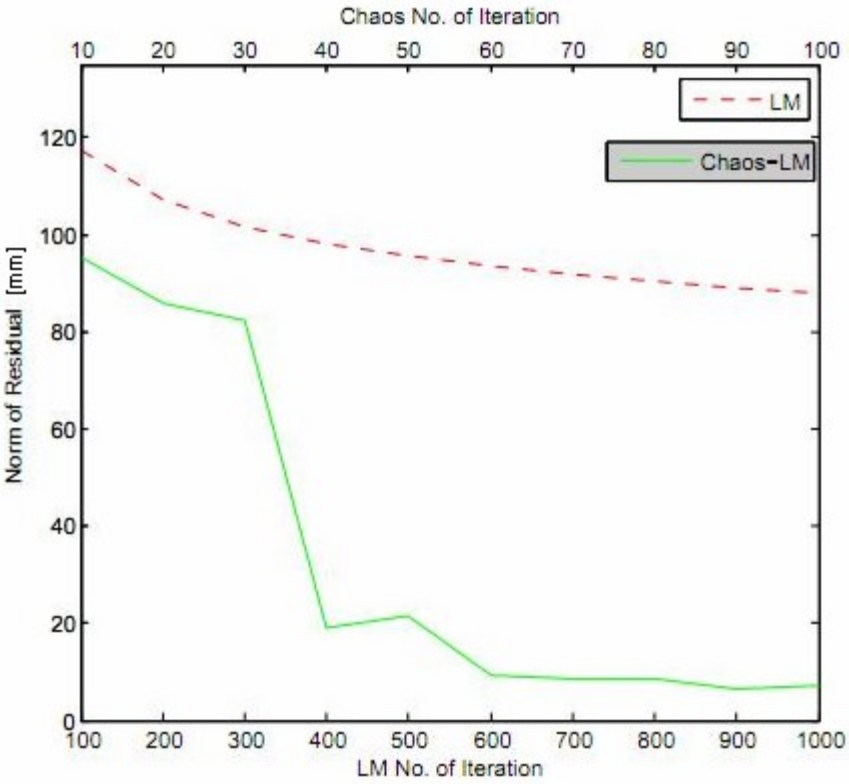

Figure 17: Convergent rate for fitting full circle point cloud.

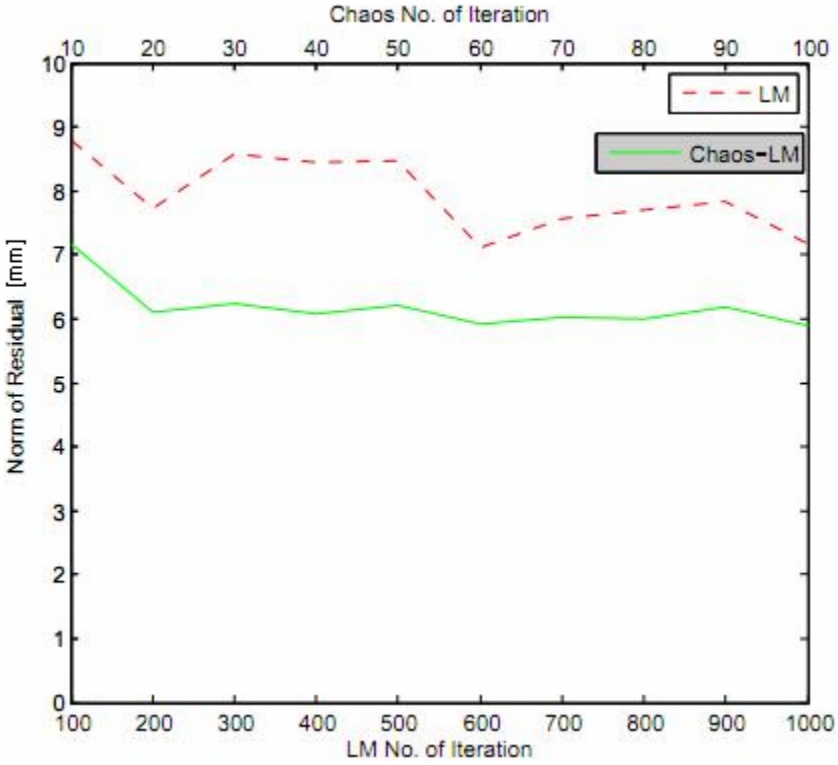

Figure 18: Convergent rate for fitting full sphere point cloud.

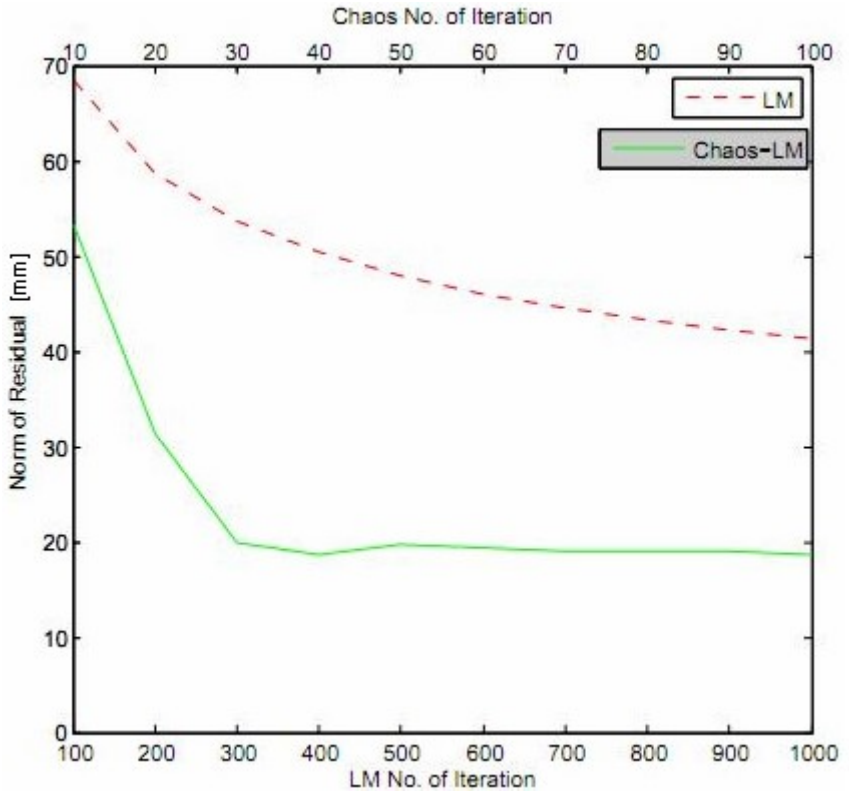

Figure 19: Convergent rate for fitting full cylinder point cloud.

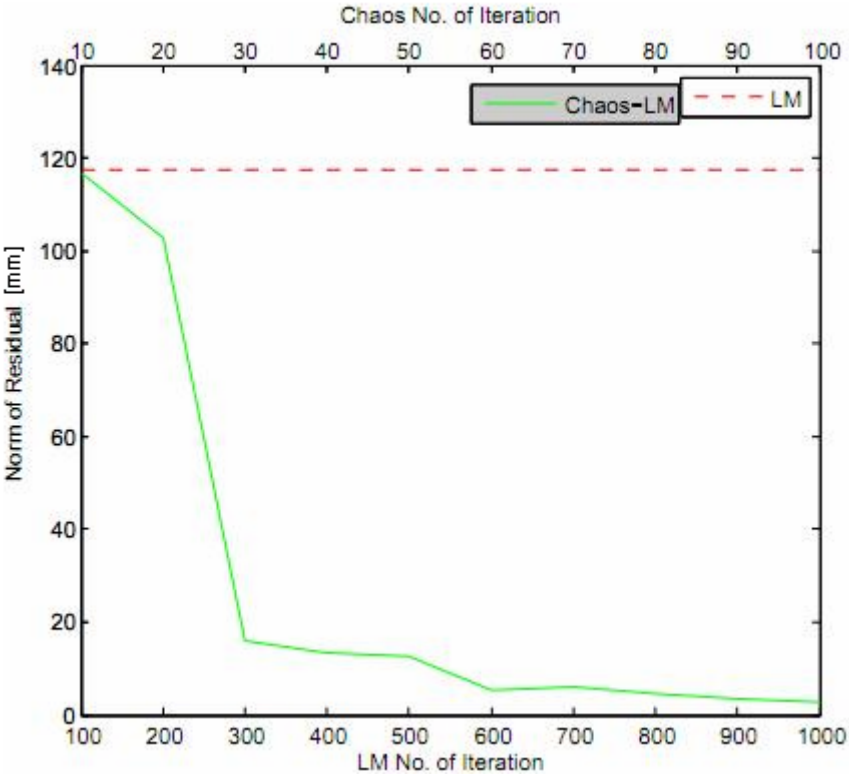

Figure 20: Convergent rate for fitting half circle point cloud.

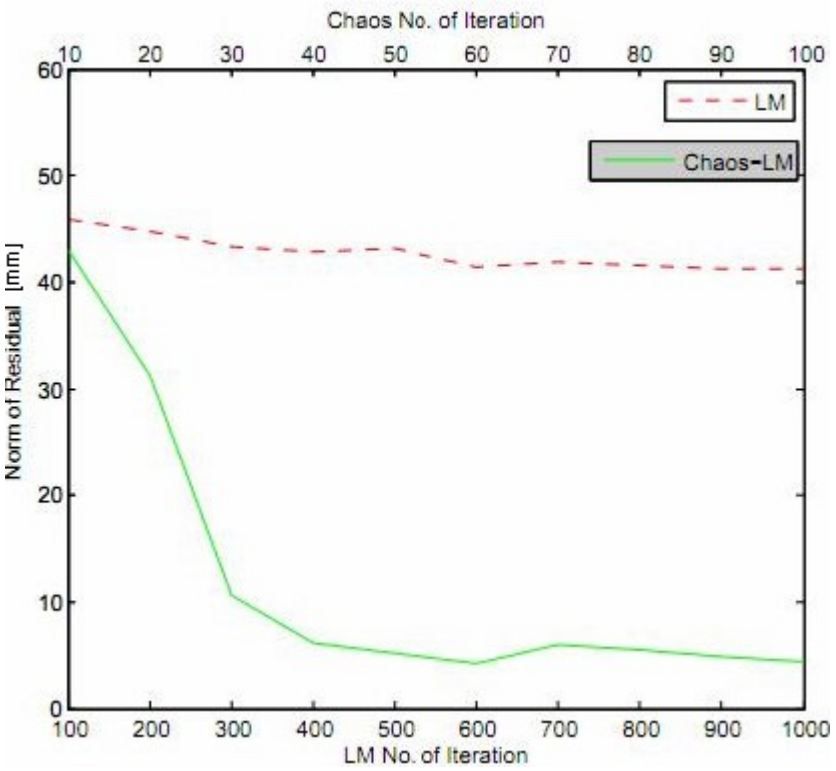

Figure 21: Convergent rate for fitting half sphere point cloud.

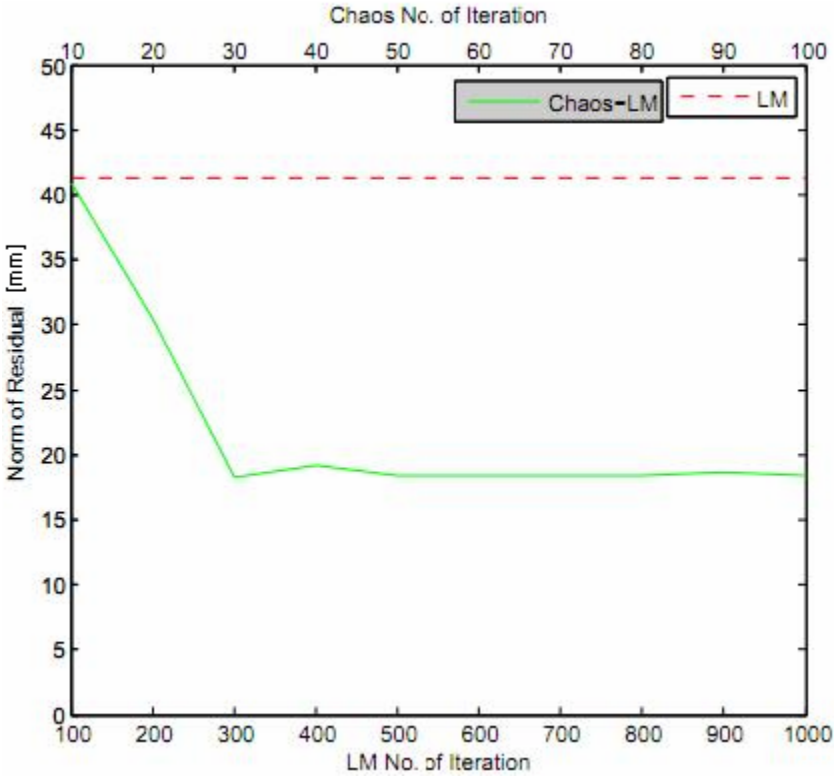

Figure 22: Convergent rate for fitting half cylinder point cloud.

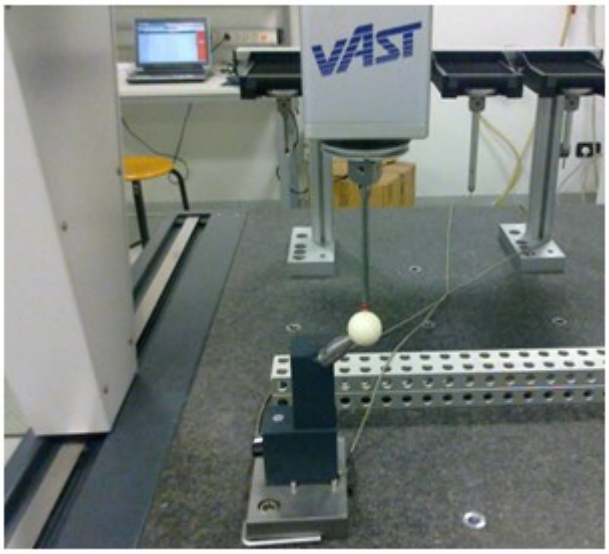

Figure 23: Measurement of calibrated ceramic sphere with Bridge-type CMM.

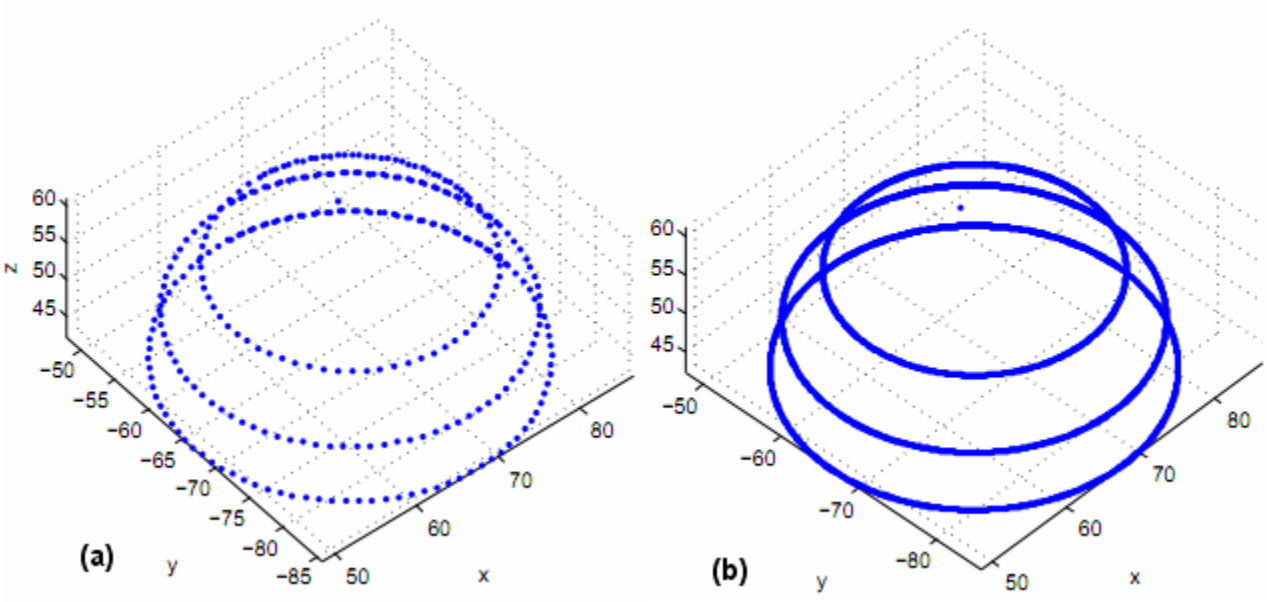

Figure 24: Obtained point cloud. (a) Low density, (b) High density.

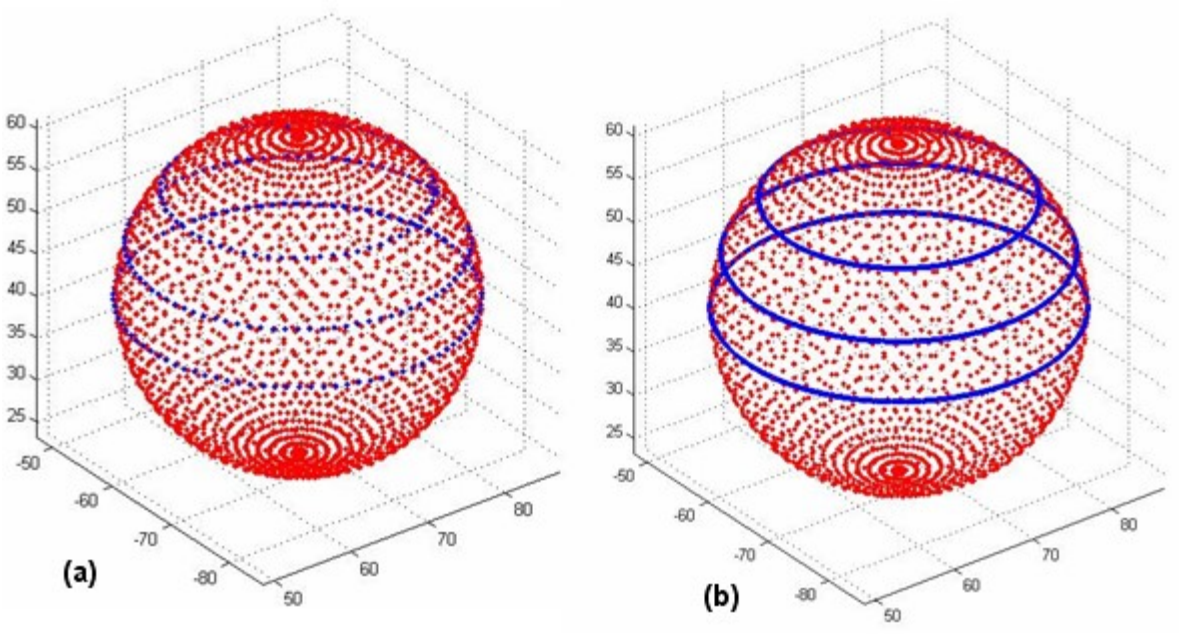

Figure 25: Sphere fitting of (a) low density, (b) high density.

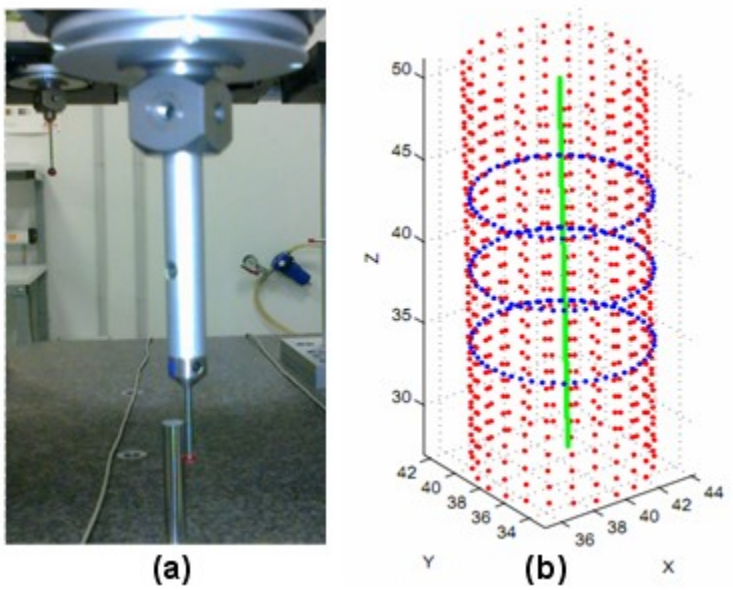

Figure 26: (a) Measurement of industrial cylinder, (b) The fitting results.